

## Freeze-form Extrusion Fabrication of Ceramics

Tieshu Huang, Michael S. Mason, Gregory E. Hilmas, and Ming C. Leu

1870 Miner Circle

Department of Materials Science & Engineering

University of Missouri – Rolla, Missouri 65409–0050

Email: {hts,mmason,ghilmas,mleu}@umr.edu

### Abstract

A novel, environmentally friendly solid freeform fabrication method called Freeze-form Extrusion Fabrication (FEF) has been developed for the fabrication of ceramic-based components. The method is based on deposition of ceramic pastes using water as the media. The ceramic solids loading can be 50 vol. % or higher and initial studies have focused on the use of aluminum oxide ( $\text{Al}_2\text{O}_3$ ). The FEF system components and their interaction are examined, and the main process parameters affecting part geometry defined. 3-D shaped components have been fabricated by extrusion deposition of the ceramic paste in a layer-by-layer fashion. The feasibility of this process has been demonstrated by building components having a simple geometry, such as cylinders and solid or hollow cones. Hollow cones have also been fabricated to demonstrate the ability to build structures with sloped walls.

### I. Introduction

Advanced ceramics are needed for applications in the aerospace, automotive, and other industries [1]. Certain ceramic materials can meet the high temperature requirements, but processing these materials into usable components is often challenging, costly, and time consuming. Being able to build a ceramic part directly by the process of material addition could considerably reduce the cost and fabrication time. Many Solid Freeform Fabrication (SFF) processes are capable of producing ceramic parts directly. One of the most extensively researched methods for rapid prototyping of ceramics is Fused Deposition of Ceramics (FDC) [2-5]. Fused Deposition Modeling (FDM) is a SFF technology developed by Stratasys (Eden Prairie, Minnesota) [5]. FDM is a layered manufacturing technique that extrudes a thin bead of plastic, one layer at a time. A thread of plastic is fed into an extrusion head, where it is heated into a semi-liquid state and extruded through a nozzle onto the previous layer of material. FDC is modified from the FDM technique by changing the deposition material from thermoplastics to a ceramic-thermoplastic mixture. FDC uses a relatively large amount of organic chemicals as binders (40-50%), providing the ability to process at low temperatures ( $< 200^\circ\text{C}$ ) and pressures ( $< 500$  psi), while solidifying rapidly to form a rigid backbone after extrusion. However, removal of organic binders produces toxic and non-decomposable wastes, which are undesirable.

In FDM, The extrusion occurs at a plastic softening temperature to form an extrudable material. Some other extrusion deposition techniques have also been investigated, for example, aqueous porcelain paste extrusion to form artificial human teeth [7] and extrusion freeform fabrication of functional graded materials [8]. In the current study, Freeze-form Extrusion Fabrication (FEF) is being combined with a previously developed Rapid Freeze Prototyping (RFP) process. RFP builds a three-dimensional ice part according to its CAD model by depositing and rapidly freezing water droplets in a layer-by-layer manner. Compared with other SFF processes, it has many advantages including less expensive equipment and material, a cleaner material and process, less energy consumption, and a better surface finish. The process for fabricating ice parts is conducted in a freezer. After being ejected from the drop-on-demand nozzle, water droplets deposit on a substrate or previously formed layer of ice. The water droplets do not solidify immediately but unite to become part of the continuous water line, which is called the water deposit. Meanwhile, the water deposit changes phase to ice in a continuous fashion [9-12].

Similar to FDC, the FEF process is also designed to use ceramic pastes with a high solids loading ( $\geq 50$  vol.%). However, the pastes use only trace amounts of organic binder (1-4%). This is possible by performing the deposition within a freezer. The lower temperatures allow the slurry to maintain its shape by freezing the water present in the slurry.

This paper will introduce the FEF process, the hardware that is currently being used, and the process parameters that affect the material deposition and the motion algorithm utilized to build hollow cone geometry. Paste behavior, freeze drying, binder removal, sintering, and materials' properties will also be detailed.

## II. Experimental Procedure

### 1. FEF equipment setup

The FEF setup is composed of five major components: the motion system, control system, deposition device, force sensor, and freezer. The following sections give a brief overview of the equipment that makes up the FEF system. Figure 1 shows the FEF system outside of the freezer.

#### 1.1. Motion system

Three extended temperature range (down to  $-40^{\circ}\text{C}$ ) stepper motors (Empire Magnetics, Rohnert Park, California) are used in conjunction with linear axes. Each linear axis has 254 mm of travel. The stepper motors have a stepping angle of 1.8 degrees, but have the ability to utilize "micro steps." The motors connected with a lead screw provide a maximum velocity of 250 mm/s and can vary their micro steps from 1-250 giving the highest resolution of 0.0072 degrees/step. In addition, the motors each have a resolver that feeds a signal to a Resolver-to-Digital converter (RDE), which converts the resolver signal into an equivalent encoder feedback, allowing for an axis resolution of  $0.5\ \mu\text{m}$  per step.

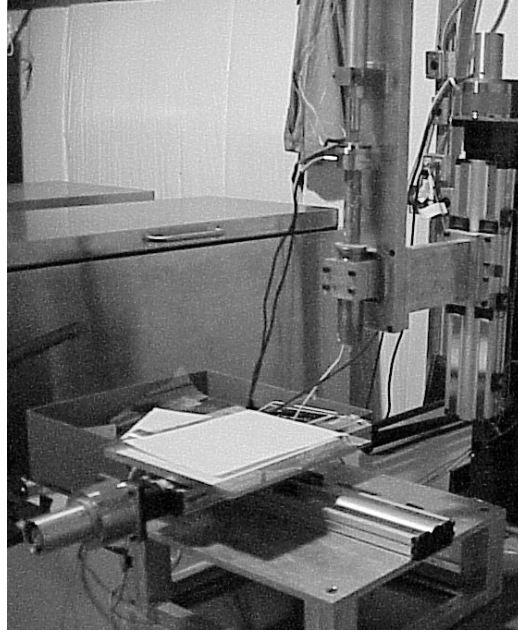


Figure 1: Freeze-form Extrusion Fabrication equipment setup

## 1.2. Real-time control system

The hardware portion of the control system is composed of a Pentium IV 3.03 GHz computer for software development and graphical user interface, which is programmed using LabView software (National Instruments, Austin, Texas). The chassis is a National Instruments PXI/SCXI 1010. The chassis has 8 slots for PXI (data acquisition and control) cards and 4 slots for SCXI (signal conditioning) cards. The cards are connected in the chassis backplane allowing for synchronous timing. The National Instruments PXI 8187 real-time controller has a dedicated 2.2 GHz processor with 1 GB of RAM and is equipped with a 30 GB hard drive, one General Purpose Interface Bus (GPIB), and two serial port connections. The controller was upgraded to an extended temperature range design due to excess heat created by the PXI cards.

A National Instruments PXI-7334 motion control card is used to regulate the motors and read the encoder feedback signals. The card can control up to 4 individual axes operated by either servo or stepper motors. The maximum pulse rate for the stepper motors is 4 MHz and the maximum encoder feedback rate is 20 MHz for each axis. There are three limits: home, forward, and reverse. The card has a trajectory loop update rate of 62.5  $\mu$ s. There are also four single ended 8 bit TTL ports for auxiliary digital communication.

A National Instruments PXI-6025E multifunction data acquisition card is used for data input and output. It has two 24 bit counter/timers, two 12 bit analog outputs, 32 digital I/O lines, and 16 analog input lines which can be used as 16 single ended or 8 double ended inputs. The maximum sampling rate is 200 kS/s per channel with the input operation range from a minimum range of -0.05 to 0.05 V up to a maximum range of -10 to 10 V.

### 1.3. Deposition device

An extrusion device (Figure 2) is necessary for deposition of ceramic pastes having a high solids loading, as the actuator can apply the necessary amount of pressure. The extrusion device is attached to the z-axis of the FEF system, and a stepper motor with a resolution of 16,000 steps/inch is used to actuate a linear axis for the extrusion process. The linear axis moves an extrusion ram, which applies pressure to a reservoir containing the paste, and ultimately to the extrusion nozzle, forcing material through the nozzle. The deposition rate can be changed by adjusting the stepper motor speed. A 60 cm<sup>3</sup> extruder reservoir is used to hold and eject the ceramic paste. Nozzles of varying diameter ranging from 190 to 580 μm are attached to the end of the extruder to allow for different diameters and thus thicknesses of material extrudate. .

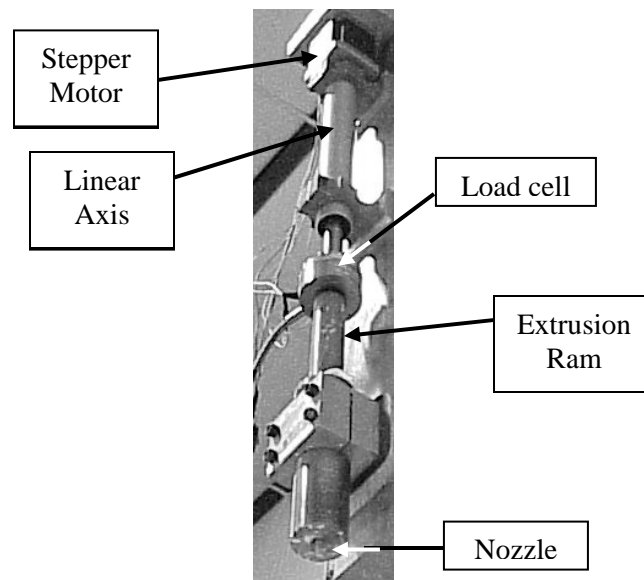


Figure 2: Extrusion device as connected to the z-axis.

### 1.4. Force sensor

A LC301-1k load cell from Omega Engineering (Stamford, Connecticut) has been implemented into the system. The load cell has been attached at the end of the extrusion linear axis. The load cell was chosen for force feedback that will allow for constant material deposition. The load cell measures the applied force of the linear axis on the extrusion ram. A differential voltage is sent by the load cell and read by the data acquisition board that corresponds to a force between 0 – 1000 lbs.

## 2. Materials and ceramic paste preparation

The materials used to form the alumina (Al<sub>2</sub>O<sub>3</sub>) based ceramic pastes in the current study are listed in Table 1. The solids loading of the pastes were from 45 ~ 55 vol.%. The solids-loading affects the rheological properties of the paste, which directly influence the extrusion behavior. Aquazol is a water soluble binder with a pH of 7, which will not affect the paste's pH

value. Binder additions of 1 ~ 4 vol.% were added to the paste to achieve consistent extrusion behavior and to assist in forming a stronger green body after drying. PEG was added as an extrusion lubricant to reduce friction between the paste and the nozzle wall as well as the friction between the particles during extrusion. Glycerol was used to prevent the growth of large ice crystals and freezing defects associated with water crystallization [13], Davan C was used as a dispersant and Deionized water as the medium.

Table 1: Materials used in paste preparation

No.	Name and Grade	Properties	Manufacturer
1	622 (A-16SG) Al <sub>2</sub> O <sub>3</sub>	APS 0.4 μm	Alcoa
2	Poly(ethylene glycol), PEG-400	MW 400	Aldrich
3	Darvan C		R. T. Vanderbilt
4	Aquazol 50	MW 50,000	ISP Technologies, Inc.
5	Glycerol		Aldrich
6	Deionized Water		

The Al<sub>2</sub>O<sub>3</sub> powder, PEG, glycerol, Darvan C, and water are mixed in a Nalgene bottle and ball milled for 24 hours using alumina milling media. Ball milling is used to break up any agglomerates in the powder to produce a uniform mixture. Aquazol is dissolved in water at 60 °C using magnetic stirring to form a 50 vol.% Aquazol solution. After ball milling the Aquazol solution is added into the batch mixture using a vacuum mixer (Whip Mix, Model F, Louisville, KY) to form a uniform paste that does not contain bubbles. The final viscosity was adjusted by adding acid to control the pH of the paste. The resulting paste is then collected into syringes and is ready for FEF processing.

### 3. Material Deposition

Path planning and material deposition are affected by three main parameters: nozzle diameter, XY table speed, and extrusion rate. Currently three different nozzle diameters have been used in this study (190, 250, 580 μm). There is a tradeoff between part build time and part accuracy that must be chosen, either a fast build time with slightly less accurate part dimensions or high dimensional accuracy with a longer build time. The extrusion rate and XY table speed must be matched in order to deposit material in a smooth continuous fashion. If the table speed is too high, the extruded material will have gaps in deposition. A high table speed creates a shearing force that overcomes the cohesion properties of the slurry. An example of this is shown in Figure 3. If the table speed is too slow then there is additional material buildup, which is undesirable for two reasons. The part accuracy is reduced do to a larger layer height and it may create the possibility of clogging the nozzle. If the nozzle is immersed in the deposited ceramic slurry for extended periods, the material starts to solidify within the nozzle thereby reducing the material flowrate and eventually causing complete clogging of the nozzle.



Figure 3: Example of gaps in material deposition

The extrusion rate is dependent upon the applied force from the extrusion ram. Force feedback is chosen to develop controllable material deposition. A load cell has been attached to the end of the extrusion ram in order to measure the amount of force being applied to the extruder. This force is fed back to the PC. A basic on/off control algorithm has been written that keeps the applied force within  $\pm 10$  lbs of the desired amount. A better control algorithm that will utilize the relationship between the extrusion velocity and applied force will be implemented later to improve material deposition.

#### 4. Freeze drying, binder removal, and sintering

Freeze drying was performed in a chamber that was set in a freezer and pumped with a mechanical vacuum pump. The freeze drying temperature was set at  $-16$  °C and the time is from 2 to 5 days in order to remove the water by sublimation, depending on the size of the sample. Following freeze drying, the samples were dried further at ambient and elevated temperatures to complete the drying process.

A thermogravimetric analyzer (Shimadzu TGA50, Lenexa, KS) was employed for determining the binder thermolysis behavior. Samples of the batched pastes were tested using a heating rate of  $5$  °C/min to  $600$  °C in air. A binder removal profile was then developed based on the thermogravimetric analysis (TGA) results and performed in a box furnace. The sintering temperature was  $1550$  °C, at a heating rate of  $5$  °C/min, and a hold time of 2 hours. Sample densities were obtained using the Archimedes method. The samples were sectioned in the direction shown in Figure 4 to check the sample uniformity, microstructure, and pore distribution using scanning electron microscopy (SEM) techniques (Jeol 330, Peabody, MA). SEM micrographs were obtained from areas a and b, as shown in Figure 4.

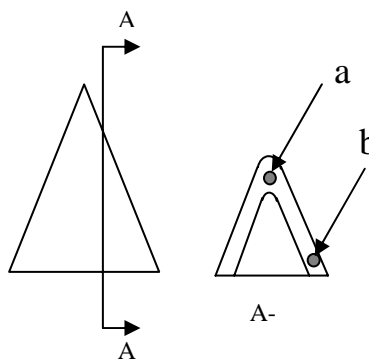


Figure 4: Schematic drawing showing the sample sectioning position and SEM analysis areas.

### III. Results and Discussion

#### 1. Rheology

Because Aquazol 50 is a neutral binder, it will not change the slurry/paste pH value when added; so the effects of dispersant content were tested prior to binder additions. The effect of binder content on viscosity of the paste was performed on batches containing 1.5 vol.% dispersant. Binder content was varied from 1 to 6 vol.% with a 1 vol.% resolution. The test results (Figure 5) show that the viscosity decreases as dispersant concentration increases when the content is less than 2 vol.%. However, the viscosity will increase as the dispersant content increases when the dispersant content is larger than 2 vol.%. It also can be determined that the slurry exhibits a strong shear thinning behavior for all ranges of dispersant content. Dispersant content of paste recipe is decided by uniform ball milling and relatively high viscosity after binder additions. The relatively high viscosity is needed for extrusion. Figure 6 shows the effect of binder content on the paste viscosity. The tendency is that the viscosity increases as the binder content increases. This effect is significant in the low shear rate region, but not as significant in the high shear rate region. 2 to 4 vol.% binder was adapted in the paste preparation procedures since these pastes exhibited a low enough viscosity in the high shear rate range to be extrudable at low pressures, while having a high enough viscosity in the low shear rate range to quickly become rigid and provide green strength after extrusion. The pH of the paste is adjustable through addition of a 4%  $\text{HNO}_3$  water solution. Test results showed that pH adjustment was the most significant method for developing a uniform paste and for controlling paste viscosity.

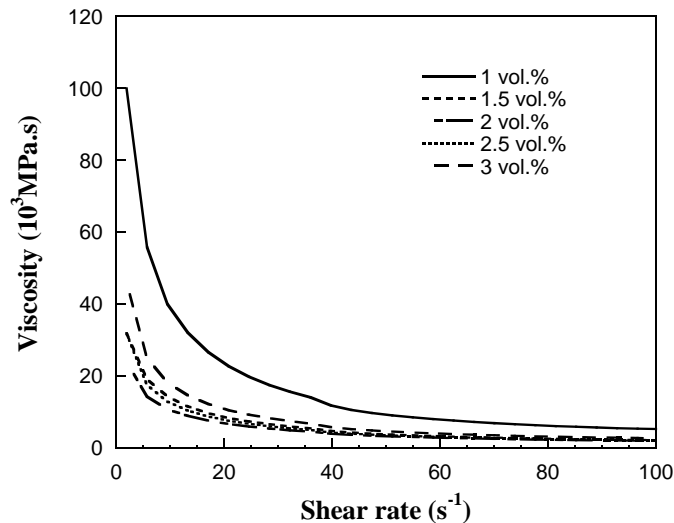


Figure 5: Effects of dispersant content on viscosity of pastes under various shear rates.

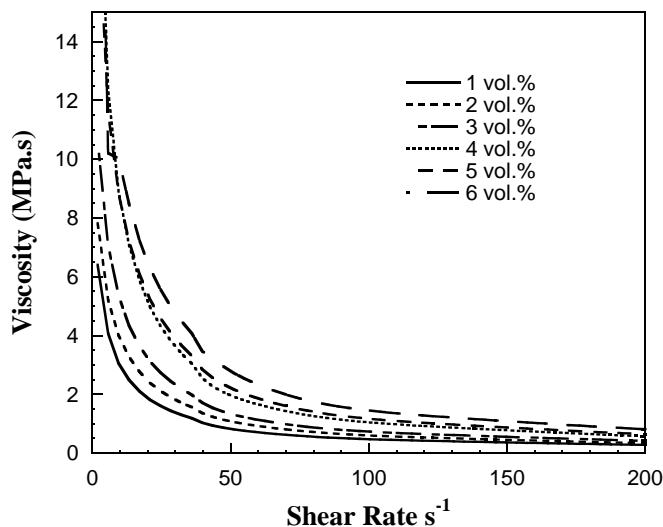


Figure 6: Effect of binder content on paste viscosity.

## 2. Fabrication of solid 3D components

Cylinders and solid cones were used to demonstrate the early stages of this developing technology (Figure 7) because they are relatively simple shapes to fabricate by SFF. The defect on the cylinder surface (Figure 7) is caused by an air bubble in the paste. The cylinder was built using a 580  $\mu\text{m}$  diameter nozzle and the solid cone was built up using a 190  $\mu\text{m}$  nozzle. In the current study, the FEF setup was not housed in a freezer due to limitations on the size of available freezers. Thus, the components in Figure 7 were built at room temperature. The rough surface in the photographs is caused by the collapse of deposited material as the component increases in size, and is due to instability of previously deposited materials. In future studies, components will be built in a freezer, resolving these issues.

## 3. Fabrication of hollow cones

In order to build hollow cone geometry, a recursive offset type of algorithm was implemented. The recursive offset algorithm moves in a trajectory that is defined by the part boundaries. More in depth information about the recursive offset algorithm can be found in [14,15]. The trajectory moves in a path along the outermost boundary first. For the hollow cone example, a counter clockwise circular movement is made. After the deposition of the boundary contour, the motion path is reduced by shifting the X axis inward by a predefined amount. This shifting value is defined by the material deposition thickness. This shifting process is repeated until the innermost boundary is reached. The innermost boundary is calculated from the wall thickness value. After the innermost boundary is deposited, a straight line vector move is performed in the XZ plane. The X axis shifts inwards a predefined amount that corresponds to the desired layer overhang value while the Z elevator moves upward by a fixed amount depending on the material deposition height. The motion is then repeated in a similar fashion for the next layer. A counterclockwise circular movement is then performed, depositing the innermost boundary followed by the X axis straight line shift with this motion repeated until the new outer boundary is reached. This combination of movements is repeated until the apex of

the cone is reached. After the top layer is finished the extrusion is stopped, the Z axis is raised, and the XY table moves away from the extrusion nozzle allowing the part to be removed. Figure 8 shows the motion for the first two layers of deposition.

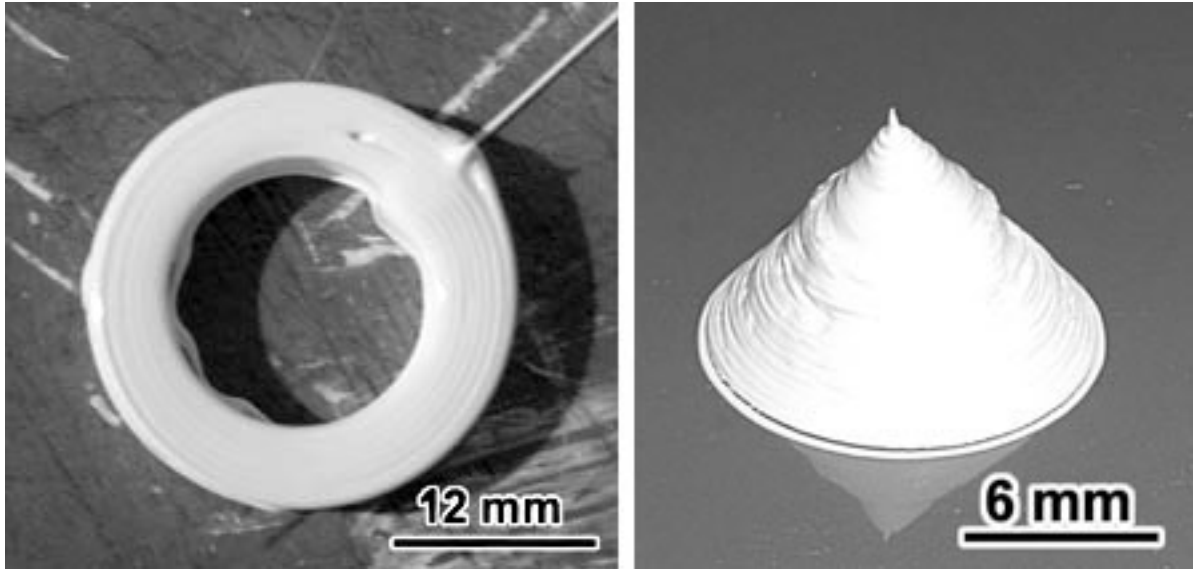


Figure 7. FEF method fabricated cylinder and solid cone.

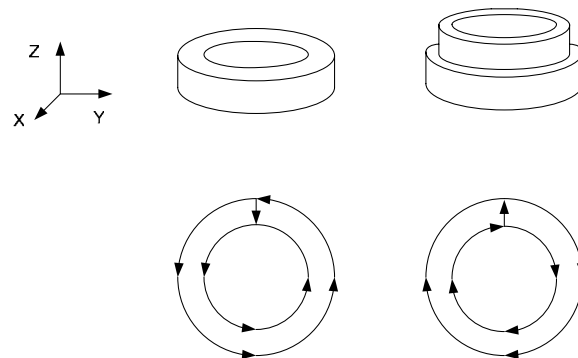


Figure 8: Motion path for the first two layers of a hollow cone

#### 4. Freeze drying, TGA, and binder removal

Successful freeze drying of highly loaded ceramic components depends on many factors. First, it depends on the vapor pressure of water at its freezing temperature. Second, it depends on the pressure of the freeze dryer. The rate of drying also depends on the geometry and surface area of the sample. Two cone samples were produced for preliminary freeze drying tests. The samples were taken directly from the deposition table, weighed immediately, and placed in the freeze dryer for two days at -16 °C under a mechanical vacuum (~1Pa).

Table 2: Freeze drying results

Sample No.	Wet Weight (g)	Dry Weight (g)	Weight Loss (%)
1	2.80	2.66	5.00
2	2.41	2.26	6.22

From the freeze drying results (Table 2), it can be seen that the mechanical vacuum pump could not meet the needs of freeze drying. Only about 30% of the water in the samples was evaporated. However, once the sample was partially freeze dried they possessed enough strength to be dried at ambient and/or elevated temperatures outside of the freeze drier. After drying, the samples were ready for binder removal. TGA results (Figure 9) show that weight loss in the samples occurs from room temperature to 600 °C in three stages. The first stage is room temperature through 120 °C. In this stage, any remaining, residual water and low melting point additives are removed. The second stage is from 120 °C to 170 °C, where glycerol is removed. The third stage is from 170 °C to 375 °C, where the higher molecular weight binders are pyrolyzed.

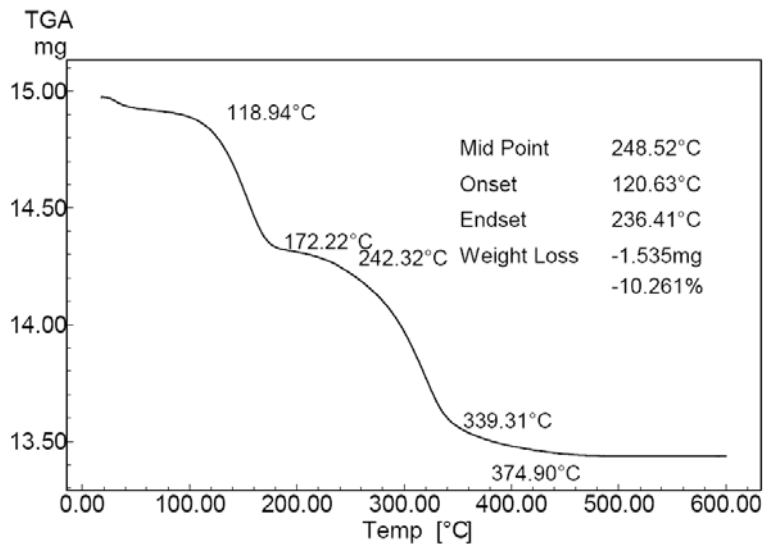


Figure 9: TGA results from a freeze dried sample.

Since the pastes in this process contain a minimum of high molecular weight organic binders, the binder removal process is relatively straightforward and can be accomplished with a

rapid heating cycle. For small samples, maximum thickness <10 mm, the binder removal can be performed using a 0.5 °C/min heating rate from room temperature to 600 °C and holding for 2 hours. The binder is completely removed under these conditions and the samples maintain their original shape.

### 5. Sintering and sample density

The schedule used for sintering the Al<sub>2</sub>O<sub>3</sub> samples in the current study was 5 °C/min ramp to 1550 °C and a hold of 2 hours. Several sintered hollow cone samples are shown in Figure 10. Archimedes density results for the samples (Table 3) show that the samples achieved an average of 90% of their theoretical density. The fairly low density is caused by under filling, resulting in gaps between the individual filaments, during material deposition and is discussed in more detail in the next section.

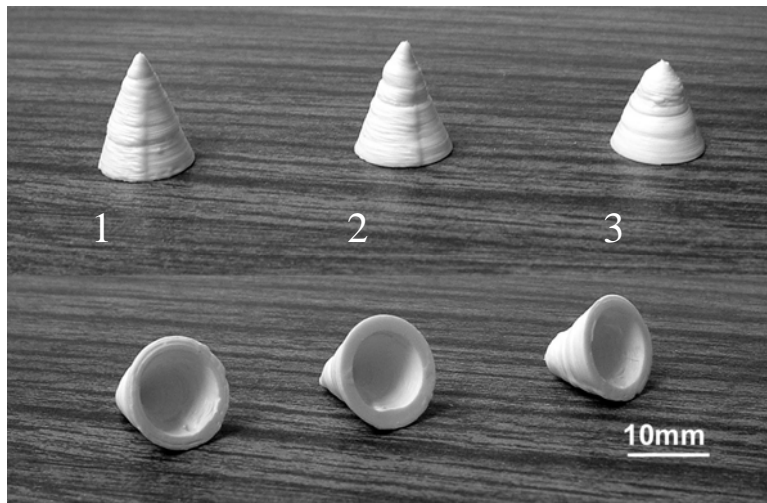


Figure 10: Optical images showing the side and bottom views of sintered hollow cones fabricated by FEF.

Table 3: Density test results

Sample No.	Density (g/cm <sup>3</sup> )	Percent of Theoretical Density
1	3.63	91
2	3.61	90
3	3.59	90
Average	3.61	90

### 6. Microstructural analysis

Figure 12 and Figure 13 are SEM images obtained from area a and area b, respectively, as shown in Figure 4. The SEM images clearly indicate that the density is not uniform from area a to area b. In area a, the density is relatively high, containing only small pores having a uniform distribution. However, in area b, the density is relatively low. Several large voids are distributed throughout the area that follows a specific pattern. According to the void distribution pattern, it is surmised that under filling of the extruded filaments occurred in this area during deposition. The under filling is caused by the mismatch of XY table velocity with the extrusion rate.

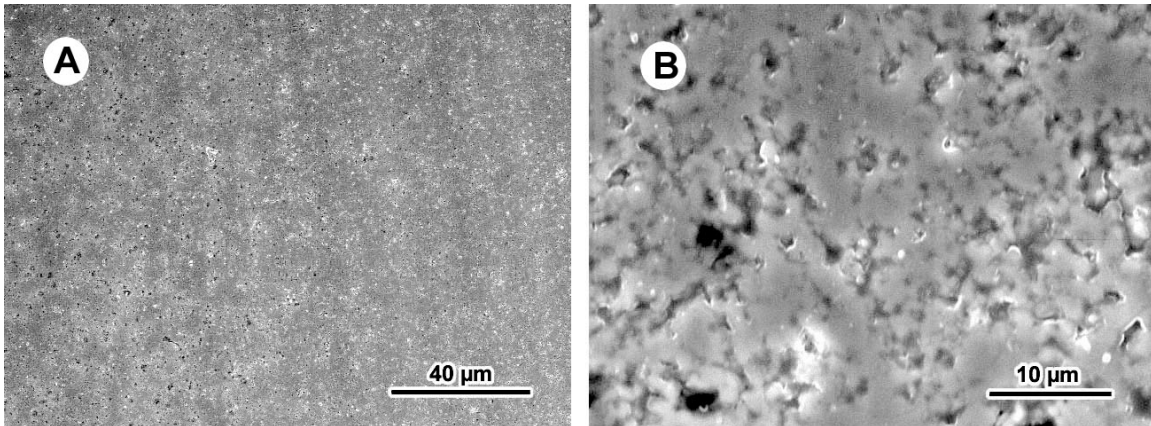


Figure 12: SEM images taken from area a (Figure 4) from a sectioned  $\text{Al}_2\text{O}_3$  hollow cone produced using FEF.

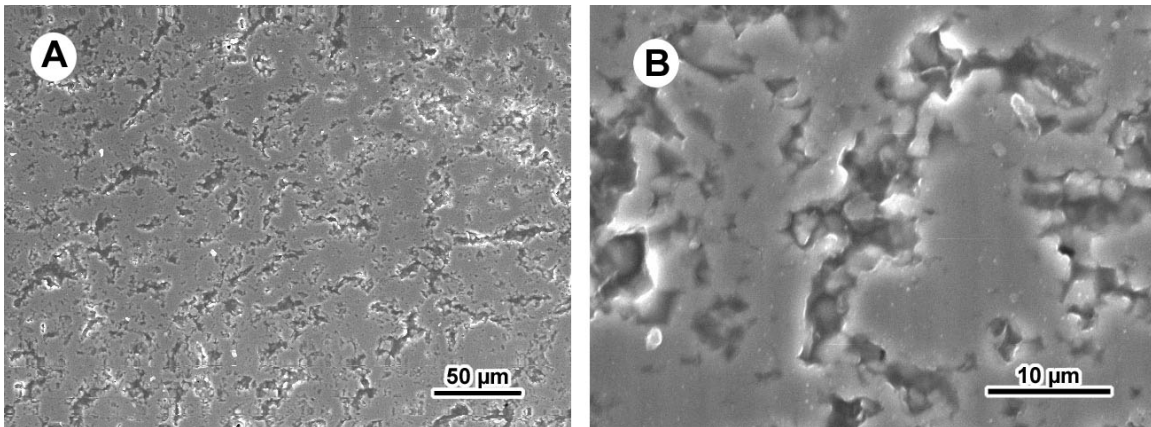


Figure 13: SEM Images taken from area b (Figure 4) from a sectioned  $\text{Al}_2\text{O}_3$  hollow cone produced using FEF.

#### IV. Conclusions

A new SFF technique called Freeze-form Extrusion Fabrication (FEF), has been developed utilizing aqueous ceramic pastes as the build material. This is an effective, time saving, and environmentally friendly solid freeform fabrication technique. The concept was tested through successful fabrication of basic 3D geometries. Aqueous pastes consisting of a 50 ~ 55 vol.% solids loading of Al<sub>2</sub>O<sub>3</sub> ceramic powder, with a minimum of organic binder content, showed favorable extrusion behavior. The dispersant, binder content and pH value strongly affected the viscosity of pastes and provided control over pasted extrusion behavior. The FEF system was described in detail and major process parameters were defined. The ability of the process to build overhanging features without the use of support material was verified through fabrication of hollow cones.

## Acknowledgement

This work was supported by the Air Force Research Laboratory under Contract FA8650-04-C-5704

## References

1. "Advanced Ceramics Technology Roadmap – Charting Our Course" Sponsored by U.S. Advanced Ceramic Association & U.S. Department of Energy, Prepared by Energetics, Inc. and Richerson and Associates, December 2000
2. S. Rangarajan, et al., "Powder Processing, Rheology, and Mechanical Properties of Feedstock for Fused Deposition of Si<sub>3</sub>N<sub>4</sub> Ceramics," *J. Am. Ceram. Soc.*, **83** [7] 1663-69 (2000).
3. G. W. Lous, et al., "Fabrication of Piezoelectric Ceramic/Polymer Composite Transducers Using Fused Deposition of Ceramics," *J. Am. Ceram. Soc.*, **83** [1] 124-28 (2000).
4. A. Bandyopadhyay, et al., "Processing of Piezocomposites by Fused Deposition Technique" *J. Am. Ceram. Soc.*, **80** [6] 1366-72 (1997).
5. U.S. Pat. No. 5738817, April 14, 1998.
6. U.S Pat No 5121329, June 1992.
7. J. W. Wang, et al., "Solid Freeform Fabrication of Artificial Human Teeth," Solid Freeform Fabrication Proceedings, pp 816-825 (2004).
8. G. E. Hilmas, et al., "Advances in the Fabrication of Functional Graded Materials using Extrusion Freeform Fabrication," Functionally Graded Materials, p319-324 (1996).
9. G. Sui, "Modeling and Analysis of Rapid Freeze Prototyping," PhD Dissertation, University of Missouri-Rolla, Rolla, Missouri. (2002).
10. F. Bryant, et al., "A Study on the Effects of Process Parameters in Rapid Freeze Prototyping," *Proceedings of Solid Freeform Fabrication Symposium*, August 5-7, Austin, Texas, pp. 635-642. (2002).
11. M. C. Leu, et al., "An Experimental and Analytical Study of Ice Part Fabrication with Rapid Freeze Prototyping," *Annals of the CIRP*, Vol. 49/1, pp. 147-150. (2000).

12. S. W. Sofie and F. Dogan, "Freeze Casting of Aqueous Alumina Slurries with Glycerol" *J. Am. Ceram. Soc.*, **84** [7] 1459-64 (2000).
13. W. Zhang, et al., "Rapid Freezing Prototyping with Water," *Materials and Design*, Vol. 20, pp. 139-145. (1999).
14. K. Eiamsa-ard, et al., "Toward Automatic Process Planning of a Multi-Axis Hybrid Laser Aided Manufacturing System: Skeleton-Based Offset Edge Generation," *Proceedings of the ASME Design Engineering Technical Conferences and Computers and Information in Engineering Conference*, September 2-6, Chicago, Illinois, Paper No. DAC-48780. (2003).
15. R. Hebbar, "Geometric Algorithms In Support of Layered Manufacturing," Ph.D. Dissertation, Stanford University Department of Electrical Engineering and Applied Physics, Stanford California. (1999).